Title: Genetic Inactivation of the β1 adrenergic receptor prevents Cerebral Cavernous Malformations in zebrafish

Authors: Wenqing Li[1,2], Sara McCurdy[1], Miguel A. Lopez-Ramirez[1], Ho-sup Lee[1], Mark H. Ginsberg[1]

[1]Department of Medicine, University of California San Diego, CA, USA

[2]To whom correspondence should be addressed

Abstract: Propranolol reduces experimental murine cerebral cavernous malformations (CCMs) and prevents embryonic caudal venous plexus (CVP) lesions in zebrafish that follow mosaic inactivation of *ccm2*. Because morpholino silencing of the β1 adrenergic receptor (*adrb1*) prevents the embryonic CVP lesion, we proposed that *adrb1* plays a role in CCM pathogenesis. Here we report that *adrb1*$^{-/-}$ zebrafish exhibited 86% fewer CVP lesions and 87% reduction of CCM lesion volume relative to wild type brood mates at 2dpf and 8-10 weeks stage, respectively. Treatment with metoprolol, a β1 selective antagonist, yielded a similar reduction in CCM lesion volume. *Adrb1*$^{-/-}$ zebrafish embryos exhibited reduced heart rate and contractility and reduced CVP blood flow. Similarly, slowing the heart and eliminating the blood flow in CVP by administration of 2,3-BDM suppressed the CVP lesion. In sum, our findings provide genetic and pharmacological evidence that the therapeutic effect of propranolol on CCM is achieved through β1 receptor antagonism.

Introduction

Cerebral cavernous malformations (CCMs), accounting for 5-15% of cerebrovascular abnormalities, are characterized by blood-filled endothelial-lined cavities, and can cause seizures, headaches, neurological deficits, and recurrent stroke risk[1]. Familial CCMs are due to heterozygous loss of function mutations in the *KRIT1, CCM2*, or *PDCD10* genes with a second mutation inactivating the normal allele in random brain endothelial cells[2]. We previously developed a zebrafish CCM model using CRISPR-Cas9 to inactivate *ccm2* in a manner that replicates the mosaic genetic background of the human disease[3]. This zebrafish model exhibits two phenotypic phases: lethal embryonic caudal venous plexus (CVP) cavernomas at 2 days post-fertilization (dpf) in ~30% of embryos and histologically-typical CNS CCMs in ~100% of surviving 8 week old fish[3]. Both phases of this model, like their murine counterpart, depend on Krüppel-like factor 2 (KLF2), confirming shared transcriptional pathways. Furthermore, both phases of the zebrafish model exhibit similar pharmacological sensitivities (Supplementary Table 1) to murine and human lesions. Thus, this zebrafish model offers a powerful tool for genetic and pharmacological analysis of the mechanisms of CCM formation.

Anecdotal case reports[4-6] and a recent phase 2 clinical trial have suggested that propranolol a non-selective β adrenergic receptor antagonist benefit patients with symptomatic CCMs[7]. In previous studies, we observed this effect of propranolol in both zebrafish and murine models of CCM[8]. Importantly, propranolol is a racemic mixture of R and S enantiomers and elegant work from the Bischoff lab has implicated the R enantiomer, which lacks β adrenergic antagonism, as the component that inhibits SOX18 thereby suppressing infantile hemangiomas[9]. We previously found that the anti-adrenergic S enantiomer rather than the R enantiomer inhibited development of embryonic CVP cavernomas in *ccm2* CRISPR zebrafish[8]. Furthermore, morpholino silencing of the gene

that encodes the β1 (*adrb1)* but not β2 *(adrb2)* receptor also prevents CVP cavernomas[8], suggesting that the β1 adrenergic receptor (β1AR), which primarily impacts hemodynamics[10], contributes to the pathogenesis of CCM. Here we have inactivated the *adrb1* gene to eliminate the β1AR and observed the expected reduction of heart rate and contractility which resulted in reduced blood flow through the CVP. These *adrb1*$^{-/-}$ zebrafish were protected from embryonic CVP cavernomas and, importantly, also exhibited much reduced number and volume of adult brain CCM. Furthermore, a β1-selective antagonist, metoprolol, also inhibited adult CCM suggesting that β1AR-specific antagonists may be useful for CCM treatment and will carry less potential for β2 AR-related side effects such as bronchospasm[11].

Results

β1AR is important in for development of CVP cavernomas

We previously reported that morpholino silencing of *adrb1* rescued CVP cavernomas in zebrafish embryos[8]. Because of morpholinos potential for off target effects[12, 13], we sought to confirm the β1AR's potential involvement in CCM pathogenesis by inactivating *adrb1.* We used CRISPR-Cas9 to generate an 8-bp deletion resulting in a premature stop codon at 57 bp (Figure 1A). To exclude potential off-target effects, the top 20 potential off-target sites predicted by Cas-OFFinder (www.rgenome.net/cas-offinder) (Supplementary Table 2) were sequenced and were not mutated (data not shown). We intercrossed *adrb1*$^{+/-}$ F1 offspring resulting in *adrb1*$^{-/-}$ zebrafish embryos that displayed reduced cardiac contractility (Supplementary Video 1) and decreased heart rate (Supplementary Figure 1A). Similar to *Adrb1*$^{-/-}$ mice[14], *adrb1*$^{-/-}$ zebrafish exhibited a blunted chronotropic response to a β1AR agonist, isoprenaline hydrochloride (Figure 1B). *Adrb1*$^{-/-}$ embryos had no obvious defects in vascular development and they survived to adulthood and were fertile.

We intercrossed *adrb*$^{+/-}$ individuals and injected one-cell stage embryos with *ccm2* CRISPR and blindly scored the presence of CVP cavernomas at 48hpf. As expected we observed CVP cavernomas in 28% of *adrb1*$^{+/+}$ embryos. In sharp contrast only 3% of *adrb1*$^{-/-}$ embryos exhibited cavernomas (Fig. 1C and D) indicating that loss of β1AR prevents CVP cavernomas. these observations demonstrate that the β1AR is required for embryonic CVP cavernoma formation.

β1AR mediates formation of adult CCM in the brain

Adult *ccm2* CRISPR zebrafish display highly penetrant CCMs throughout the central nervous system[3]. Brains from adult *ccm2* CRISPR fish on *adrb1*$^{-/-}$ (12 brains) or wild type (13 brains) background were treated with CUBIC (clear, unobstructed brain/body imaging

cocktails and computational analysis)[15], and these transparent brains were then scanned with light-sheet microscopy and lesions were enumerated and volumes were estimated with NIH ImageJ. While the typical multi-cavern CCMs were observed in brains on wild type background appearing as blood filled dilated vessels (Figure 2A through C), *ccm2* CRISPR *adrb1*$^{-/-}$ fish exhibited an 87% reduction in lesion volume (Figure 2D through G). Thus, genetic inactivation of β1AR prevented CCMs.

A selective β1AR antagonist prevents CCMs

The non-selective β blocker propranolol reduces lesion volume in murine CCM models[8, 16]. To ascertain whether propranolol had a similar effect in the zebrafish model, the chemical treatment was started from larval stage at concentration which allows the fish to develop to two months for CCM inspection. We added 12.5μM propranolol to or vehicle control to fish water of *ccm2* CRISPR zebrafish starting at 3 weeks of age. The water was refreshed daily with drug or vehicle until fish were sacrificed and brains were examined as described (Figure 3A). Quantification based on light-sheet scanning of zebrafish brains (Figure 3B) showed that compared to vehicle-treated controls (Figure 3C, D, and E), propranolol-treated groups displayed a 94% reduction in CCM lesion volume (Figure 3F, G, and H). Similarly, administration of 50μM racemic metoprolol a β1-selctive antagonist produced a similar (98%) reduction in lesion volume (Figure 3B, I, J, and K). Importantly, neither drug at the doses administered reduced the growth of the fish or the volume of their brains. In sum, both genetic and pharmacological loss of β1 adrenergic receptor signaling markedly reduces the lesion burden in the zebrafish *ccm2* CRISPR model of CCM.

Loss of β1AR does not prevent increased *klf2a* expression in *ccm2* null embryos

Inactivation of CCM genes leads to increased endothelial KLF2 expression[17, 18], a transcription factor important in cavernoma formation[3, 19]. Nevertheless, silencing of *adrb1* did not prevent the expected increased endothelial *klf2a*[17] expression in *ccm2* morphant *Tg(klf2a:H2b-EGFP)* fish in which the nuclear EGFP expression is driven by the *klf2a* promoter (Figure 4A, B and C). We previously reported that mosaic expression of KLF2a occurs in *tnnt* morphant 2 dpf *ccm2* CRISPR embryos, as judged by a widely variable in endothelial *klf2a* reporter expression[3]. Nevertheless, combination of *tnnt2a* morphant with the *adrb1* morphant (Figure 4D) or control morphant (Figure 4E) *ccm2* CRISPR *Tg(klf2a:H2b-EGFP)* embryos both displayed a similar widely variable *klf2a* reporter intensity (Figure 4F) indicative of similar mosaicism. Similarly, merely slowing the heart and reducing contractility with 2,3-butanedione monoxime (BDM)[20] also prevented CVP cavernomas (Fig 4G, and Supplementary Figure 2). Thus, silencing β1AR does not prevent the generalized increase in endothelial KLF2a in *ccm2* morphants nor does it prevent the mosaic KLF2a increase in *ccm2* CRISPR zebrafish.

Discussion

In this study, we provide genetic and pharmacological evidence to implicate the β1 adrenergic receptor (β1AR) in the pathogenesis of CCM. Our data suggest that inactivating β1AR via gene inactivation or pharmacological inhibition can significantly reduce the volume of CCM lesions in a zebrafish model.

Case reports[4-6, 21] and our previous study[8] revealed the potential benefit of the non-selective β-adrenergic receptor blocker propranolol in reducing CCMs in patients and mouse models, respectively. However, propranolol is a racemic mixture, and its R enantiomer which lacks β-adrenergic antagonism was reported to show therapeutic effect for infantile hemangiomas in an animal study[9]. Notably, our study demonstrates that *adrb1*$^{-/-}$ zebrafish are significantly protected against the formation of CCMs, suggesting that propranolol's therapeutic effect on CCM is through β1AR antagonism. Together with the observed significant reduction of CCM lesion volume upon metoprolol treatment, a selective β1AR antagonist, supports the therapeutic potential of β1AR antagonism in CCMs. β1 selective blockers offer the advantage of causing fewer mechanism-based side effects compared to propranolol, such as bronchospasm[22], and are already in clinical use (including agents like atenolol, metoprolol, nebivolol, and bisoprolol). Thus, further studies are warranted to evaluate the potential value of β1 selective antagonists in this disease.

Consistent with the *Adrb1KO* mice[14], the *adrb1*$^{-/-}$ zebrafish embryos displayed the decreased chronotropic response to a beta-adrenergic agonist, isoprenaline, and decreased basal heart rate compared to that of *adrb1*$^{+/+}$ brood mates; however, CVP morphology of *adrb1*$^{-/-}$ embryo was not perturbed (Supplementary Figure 3). *adrb1*$^{-/-}$ embryo also displayed a marked decrease of blood flow in CVP (Supplementary Video 2, and Supplementary Figure 1B), A similar reduction of heart rate and contractility by 2,3-BDM, a cardiac myosin ATPase inhibitor, prevented CVP dilation (Figure.4F). We

previously found that arresting blood flow prevents aberrant intussusceptive angiogenesis and the resulted CVP cavernomas in *ccm2* CRISPR embryos[3]. Taken together, these data suggest that reduced blood flow secondary to reduced cardiac function accounts for the protective effect of loss of β1AR signaling on CVP lesions and on CCM. To further confirm that reduced blood flow underlies the role of β1AR antagonism in rescuing these vascular defects, chemicals such as cardiac glycosides or phosphodiesterase inhibitors could be employed to restore cardiac pumping function in *adrb1*$^{-/-}$ embryos. Importantly, although β1AR are highly expressed in cardiomyocytes and contribute to increased cardiac output[23], β1ARs are also expressed in other tissues[24, 25] including endothelial cells of vascular anomalies in patients[26]. Thus, future studies will be required to delineate the tissue-specific contributions of β1AR signaling to CCM pathogenesis.

Experimental procedures

Zebrafish lines and handling

Zebrafish were maintained and with approval of Institutional Animal Care and Use Committee of the University of California, San Diego. The following mutant and transgenic lines were maintained under standard conditions: *Tg(fli1:EGFP)*^{y1} [27], *Tg(klf2a:H2b-EGFP)* [28], and *Tg(kdrl:mcherry)*^{is5} [29]. *adrb1*$^{-/-}$ zebrafish was obtained by coninjection of Cas9 protein (EnGen Spy Cas9 NLS, M0646, NEB) with gRNA targeting *adrb1*. Genotyping of *adrb1*$^{-/-}$ was performed with forward primer (5'-AGAGCAGAGCGCGGATGGAA-3') and reverse primer (5'-GATCCATACATCCAGGCT-3').

Plasmids and morpholino

pCS2-nls-zCas9-nls (47929) and pT7-gRNA (46759) were bought from Addgene. The CRISPR RNA (crRNA) sequences used in this study are as follow: *ccm2*-1 5'-GGTGTTTCTGAAAGGGGAGA-3', *ccm2*-2 5'- GGAGAAGGGTAGGGATAAGA-3', *ccm2*-3 5'-GGGTAGGGATAAGAAGGCTC-3', *ccm2*-4 5'-GGACAGCTGACCTCAGTTCC-3', adrb1 5'-GACTCTAAACGCGCCACGG-3'. Target gRNA constructs were generated as described before[30]. Morpholino sequence used in this study are: *adrb1* (5'-ACGGTAGCCCGTCTCCCATGATTTG-3')[31], *ccm2* (5'-GAAGCTGAGTAATACCTTAA CTTCC-3')[32], *tnnt2a* (5'-CATGTTTGCTCTGATCTGACACGCA-3')[33], control (5'-CCTCTTACCTCAGTTACAATTTATA-3').

RNA synthesis

The pCS2-nls-zCas9-nls plasmid containing Cas9 mRNA was digested with NotI enzyme, followed by purification using a Macherey-Nagel column, serving as the template. The capped nls-zCas9-nls RNA was synthesized using the mMESSAGE mMACHINE SP6 Transcription Kit from ThermoFisher Scientific. The resulting RNA was purified through lithium chloride precipitation, as per the instructions provided in the kit. For gRNA

synthesis, the gRNA constructs were linearized using BamHI enzyme and purified using a Macherey-Nagel column. The gRNA was synthesized via in vitro transcription using the MEGAshortscript T7 Transcription Kit from ThermoFisher Scientific. After synthesis, the gRNA was purified by alcohol precipitation, as instructed in the same kit. The concentration of the nls-zCas9-nls RNA and gRNA was measured using a NanoDrop 1000 Spectrophotometer from ThermoFisher Scientific, and their quality was confirmed through electrophoresis on a 1% (wt/vol) agarose gel.

Microinjection

All injections were performed at 1-cell stage with a volume of 0.5nl. The final injection concentrations are as follow: Cas9 protein (10μM), Cas9 mRNA (750ng/μl), gRNA 120ng/μl, *adrb1* MO (4ng/μl), *ccm2* MO (4ng/μl), *tnnt2a* MO (5.3 ng/μl), control MO (4ng/μl).

Chemical treatment

Propranolol (P0995, TCI) (12.5μM) and metoprolol (M1174, Spectrum) (50μM) were used to treat the zebrafish larva from Day 21. Beginning from Day 35, adjusted concentration of propranolol (25μM) or metoprolol (100μM) were used to treat the juvenile fish. The chemicals were dissolved in fish water, and fish water containing chemicals were refreshed daily. Egg water without above chemicals was refreshed daily for fish used as negative control. 2,3- butanedione monoxime (BDM) (6mM) was added to egg water of the *ccm2* CRISPR embryos at 25hpf, and CVP cavernoma was observed at 2dpf.

Airyscan imaging and fluorescence intensity analysis

To prepare the embryos for imaging, they were first anesthetized using egg water containing 0.016% tricaine (3-amino benzoic acid ethyl ester) from Sigma-Aldrich. Subsequently, the anesthetized embryos were embedded in 1% low melting point agarose obtained from Invitrogen (product number 16520050). The imaging process was carried

out using a Zeiss 880 Airyscan confocal microscope, utilizing the standard Airyscan stack mode, with a Plan-Apochromat 20x/0.8 M27 objective. The scanning setup is as follow: Lasers (Green 488nm: 26.0%, Red 561nm: 15.0%), Master Gain (800), Digital Gain (1.00), Scaling X (0.415µm), Scaling Y (0.415µm), and Scaling Z (0.800µm). The intensity of nuclear EGFP (enhanced green fluorescent protein) was quantified using ImageJ software. The selected background area signal was measured by running Analyze>Measure. Then the background value was subtracted by running Process>Math>Subtract. "Freehand selections" button was used for outlining the endothelial nucleus stack by stack along Z-axis. By running Analyze>Measure, the information of "Area" and "IntDen (Integrated Density)" of the selected endothelial nucleus was obtained. The average EGFP intensity of a nucleus equals to the summation of "IntDen" divided by summation of "Area".

Heartbeat and blood flow recording

Heartbeat and blood flow were recorded using Olympus MVX10. The embryos were treated with 0.004% tricaine which does not have effect on heartbeat[34, 35].

Zebrafish brain dissection, CUBIC treatment and lightsheet imaging

The dissection of zebrafish brains followed the methodology described in a previous study by Gupta et al.[36]. The CUBIC method was optimized based on the findings from a previous report by Susaki et al.[15]. The brains were fixed in 4% paraformaldehyde (PFA) with a pH of 7.5 for 24 hours and subsequently washed with PBS (phosphate-buffered saline) for an additional 24 hours. Following the PBS wash, the brains underwent CUBICR1 treatment at 37°C in a water bath for 42 hours. For imaging, the samples were placed in CUBICR2 as the imaging medium and imaged using a ZEISS Lightsheet Z.1 microscope. Scanning was carried out utilizing 5X dual illumination optics in combination with a 5X objective.

Statistical analysis

The statistical analysis was conducted using GraphPad Prism software. P-values were calculated using an unpaired two-tailed Student's t-test, unless otherwise specified. The bar graphs display the mean values along with their corresponding standard deviations (SD).

Figure legends

Figure 1. Adrb1 signaling is essential for CVP dilation. (A) The targeted *adrb1* allele shows an 8-nucleotide deletion producing a pre-stop codon. *Adrb1* null cDNA is predicted to encode truncated adrb1 protein. The wild type adrb1 protein contains 390 amino acids, while the predicted adrb1 null protein would contain 2 missense amino acids (gray bar) and would terminate after amino acid 18. (B) Isoprenaline hydrochloride (50 μM) treatment at 72hpf lead to a heart rate increase in zebrafish, while the delta heart rate in *adrb1*$^{-/-}$ is significantly smaller than that of wild type. Heartbeat was counted in 18 embryos of each group before and immediately after adding the chemical. Paired two-tailed t test, P<0.0001. (C) After *ccm2* CRISPR injection, representative bright field and confocal images of 2dpf *Tg(fli1:EGFP)* embryos show that wild type embryos display CVP dilation, while *adrb1*$^{-/-}$ embryos were resistant to this defect. Arrowhead and arrows indicate the dilation in CVP. Scale bar: 500 μm (bright field), 100μm (confocal). (D) Paired two-tailed t test shows that percentage of embryos displaying CVP dilation is significantly smaller on *adrb1*$^{-/-}$ background than that of control embryos. P=0.0012. 345 *adrb1*$^{-/-}$ embryos and 237 control embryos from 4 experiments were examined for CVP cavernoma.

Figure 2. Genetic inhibition of adrb1 signaling could rescue CCM in *ccm2* CRISPR zebrafish. (A through F) Representative light sheet microscopy scanning pictures of brains from *ccm2* CRISPR adult zebrafish of *adrb1*$^{+/+}$ (A through C) and of *adrb1*$^{-/-}$ (D through F) on *Tg(fli1:EGFP)* background. Brains from *ccm2* CRISPR on wild type background show lesions indicated by arrows (A through C), while brains from *ccm2* CRISPR on *adrb1*$^{-/-}$ do not show lesions (D through F). Scale bar: 1mm. (G) Statistical analysis of total lesion volume by unpaired two-tailed t test. P=0.0005. 12 *adrb1*$^{-/-}$ brains and 13 *adrb1*$^{+/+}$ brains were analyzed.

Figure 3. Both propranolol and metoprolol could rescue CCM in *ccm2* CRISPR zebrafish. (A) A diagram outlines the drug treatment experiment, CUBIC treatment and following recording of CCMs in adult zebrafish brain. The chemical treatment was started from week 3 with 12.5 µM propranolol or 50 µM metoprolol, and increased to 25 µM propranolol and 100 µM metoprolol, respectively from week 5. The fish water with chemicals or vehicle control are refreshed on a daily basis. (B) Statistical analysis of lesion volume by one-way ANOVA followed by Tukey's multiple comparison test. P<0.01. 12 propranolol treated, 12 metoprolol treated, and 13 vehicle brains were analyzed. (C through K) Representative light sheet microscopy scanning pictures of brains from *ccm2* CRISPR adult zebrafish on *Tg(fli1:EGFP)* background. In controls without chemical treatment (C, D, and E) there were vascular anomalies indicated by arrows. Neither propranolol (F, G, and H) nor metoprolol (I, J, and K) treated fish showed vascular lesions in the brain. Scale bar: 1mm.

Figure 4. Adrb1 signaling does not alter *klf2a* expression in *ccm2* CRISPR embryos. *Tg(klf2a:H2b-EGFP; kdrl:mcherry)* embryos were injected and nuclear EGFP signal in mcherry labeled vascular endothelial cells is recorded by confocal. Representative images from each group are shown. (A) Control MO alone injected embryos were used as control. (B and C) *Ccm2* morphant embryos co-injected with *adrb1* MO (B) or control MO (C) both displayed significant increase of endothelial nuclear EGFP intensity (P<0.0001) compared to that of control (A), and there is no significant difference between them. (D and E) All the *ccm2* CRISPR embryos were co-injected with *tnnt* MO, which are absent of blood flow. Compared to that of control (A), *ccm2* CRISPR embryos co-injected with *adrb1* MO (D) or control MO (E) both displayed a mosaic increase of nuclear EGFP intensity of vascular endothelial cells compared to control (A) (P<0.0001), and there is no significant difference between them. Arrows indicated the endothelial nuclei with significant higher EGFP intensity than those indicated by arrowheads. Scale bar:100µm. (F) EGFP intensity of

endothelial nuclei were quantified with Image J. The number of analyzed nuclei were: 63 from 10 embryos (control MO), 70 from 10 embryos (*ccm2* MO+*adrb1* MO), 77 from 10 embryos (*ccm2* MO+control MO), 93 from 13 embryos (*ccm2* CRISPR+*adrb1* MO), and 94 from 13 embryos (*ccm2* CRISPR+control MO). Statistical analysis is performed by one-way ANOVA followed by Tukey's multiple comparison test. (G) At 2dpf, 2,3-BDM prevented the CVP cavernoma dramatically. 164 embryos in 2,3-BDM treated group and 177 in control group were used for Two-tailed paired t-test. P=0.0013.

Acknowledgements

We gratefully acknowledge Douglas A Marchuk, and Issam A. Awad for their invaluable advice on both this study and the manuscript. This work was supported by NIH grants P01 NS092521 and P01 HL151433. We also acknowledge Jennifer Santini and Marcy Erb for microscopy technical assistance and resources provided by the UCSD School of Medicine Microscopy Core (NINDS P30 NS047101).

Literature Cited

1. Leblanc GG, Golanov E, Awad IA, Young WL and Biology of Vascular Malformations of the Brain NWC. Biology of vascular malformations of the brain. *Stroke*. 2009;40:e694-702.
2. Labauge P, Denier C, Bergametti F and Tournier-Lasserve E. Genetics of cavernous angiomas. *Lancet Neurol*. 2007;6:237-44.
3. Li W, Tran V, Shaked I, Xue B, Moore T, Lightle R, Kleinfeld D, Awad IA and Ginsberg MH. Abortive intussusceptive angiogenesis causes multi-cavernous vascular malformations. *Elife*. 2021;10.
4. Goldberg J, Jaeggi C, Schoeni D, Mordasini P, Raabe A and Bervini D. Bleeding risk of cerebral cavernous malformations in patients on beta-blocker medication: a cohort study. *J Neurosurg*. 2018:1-6.
5. Moschovi M, Alexiou GA, Stefanaki K, Tourkantoni N and Prodromou N. Propranolol treatment for a giant infantile brain cavernoma. *J Child Neurol*. 2010;25:653-5.
6. Reinhard M, Schuchardt F, Meckel S, Heinz J, Felbor U, Sure U and Geisen U. Propranolol stops progressive multiple cerebral cavernoma in an adult patient. *J Neurol Sci*. 2016;367:15-7.
7. Lanfranconi S, Scola E, Meessen J, Pallini R, Bertani GA, Al-Shahi Salman R, Dejana E, Latini R and Treat CCMI. Safety and efficacy of propranolol for treatment of familial cerebral cavernous malformations (Treat_CCM): a randomised, open-label, blinded-endpoint, phase 2 pilot trial. *Lancet Neurol*. 2022.
8. Li W, Shenkar R, Detter MR, Moore T, Benavides C, Lightle R, Girard R, Hobson N, Cao Y, Li Y, Griffin E, Gallione C, Zabramski JM, Ginsberg MH, Marchuk DA and Awad IA. Propranolol inhibits cavernous vascular malformations by beta1 adrenergic receptor antagonism in animal models. *J Clin Invest*. 2021;131.
9. Overman J, Fontaine F, Wylie-Sears J, Moustaqil M, Huang L, Meurer M, Chiang IK, Lesieur E, Patel J, Zuegg J, Pasquier E, Sierecki E, Gambin Y, Hamdan M, Khosrotehrani K, Andelfinger G, Bischoff J and Francois M. R-propranolol is a small molecule inhibitor of the SOX18 transcription factor in a rare vascular syndrome and hemangioma. *Elife*. 2019;8.
10. van den Meiracker AH, Man in't Veld AJ, Boomsma F, Fischberg DJ, Molinoff PB and Schalekamp MA. Hemodynamic and beta-adrenergic receptor adaptations during long-term beta-adrenoceptor blockade. Studies with acebutolol, atenolol, pindolol, and propranolol in hypertensive patients. *Circulation*. 1989;80:903-14.
11. Maclagan J and Ney UM. Investigation of the mechanism of propranolol-induced bronchoconstriction. *Br J Pharmacol*. 1979;66:409-18.
12. Robu ME, Larson JD, Nasevicius A, Beiraghi S, Brenner C, Farber SA and Ekker SC. p53 activation by knockdown technologies. *PLoS Genet*. 2007;3:e78.
13. Eisen JS and Smith JC. Controlling morpholino experiments: don't stop making antisense. *Development*. 2008;135:1735-43.
14. Rohrer DK, Desai KH, Jasper JR, Stevens ME, Regula DP, Jr., Barsh GS, Bernstein D and Kobilka BK. Targeted disruption of the mouse beta1-adrenergic receptor gene: developmental and cardiovascular effects. *Proc Natl Acad Sci U S A*. 1996;93:7375-80.
15. Susaki EA, Tainaka K, Perrin D, Yukinaga H, Kuno A and Ueda HR. Advanced CUBIC protocols for whole-brain and whole-body clearing and imaging. *Nat Protoc*. 2015;10:1709-27.
16. Oldenburg J, Malinverno M, Globisch MA, Maderna C, Corada M, Orsenigo F, Conze LL, Rorsman C, Sundell V, Arce M, Smith RO, Yau ACY, Billstrom GH, Magi CO, Beznoussenko GV, Mironov AA, Fernando D, Daniel G, Olivari D, Fumagalli F, Lampugnani MG, Dejana E and Magnusson PU. Propranolol Reduces the Development of Lesions and Rescues Barrier Function in Cerebral Cavernous Malformations: A Preclinical Study. *Stroke*. 2021;52:1418-1427.

17. Renz M, Otten C, Faurobert E, Rudolph F, Zhu Y, Boulday G, Duchene J, Mickoleit M, Dietrich AC, Ramspacher C, Steed E, Manet-Dupe S, Benz A, Hassel D, Vermot J, Huisken J, Tournier-Lasserve E, Felbor U, Sure U, Albiges-Rizo C and Abdelilah-Seyfried S. Regulation of beta1 integrin-Klf2-mediated angiogenesis by CCM proteins. *Dev Cell*. 2015;32:181-90.
18. Zhou Z, Rawnsley DR, Goddard LM, Pan W, Cao XJ, Jakus Z, Zheng H, Yang J, Arthur JS, Whitehead KJ, Li D, Zhou B, Garcia BA, Zheng X and Kahn ML. The cerebral cavernous malformation pathway controls cardiac development via regulation of endocardial MEKK3 signaling and KLF expression. *Dev Cell*. 2015;32:168-80.
19. Zhou Z, Tang AT, Wong WY, Bamezai S, Goddard LM, Shenkar R, Zhou S, Yang J, Wright AC, Foley M, Arthur JS, Whitehead KJ, Awad IA, Li DY, Zheng X and Kahn ML. Cerebral cavernous malformations arise from endothelial gain of MEKK3-KLF2/4 signalling. *Nature*. 2016;532:122-6.
20. Bartman T, Walsh EC, Wen KK, McKane M, Ren J, Alexander J, Rubenstein PA and Stainier DY. Early myocardial function affects endocardial cushion development in zebrafish. *PLoS Biol*. 2004;2:E129.
21. Miquel J, Bruneau B and Dupuy A. Successful treatment of multifocal intracerebral and spinal hemangiomas with propranolol. *J Am Acad Dermatol*. 2014;70:e83-e84.
22. Ji Y, Chen S, Wang Q, Xiang B, Xu Z, Zhong L, Yang K, Lu G and Qiu L. Intolerable side effects during propranolol therapy for infantile hemangioma: frequency, risk factors and management. *Sci Rep*. 2018;8:4264.
23. Rohrer DK, Chruscinski A, Schauble EH, Bernstein D and Kobilka BK. Cardiovascular and metabolic alterations in mice lacking both beta1- and beta2-adrenergic receptors. *J Biol Chem*. 1999;274:16701-8.
24. Guimaraes S and Moura D. Vascular adrenoceptors: an update. *Pharmacol Rev*. 2001;53:319-56.
25. Osswald W and Guimaraes S. Adrenergic mechanisms in blood vessels: morphological and pharmacological aspects. *Rev Physiol Biochem Pharmacol*. 1983;96:53-122.
26. Stanciulescu MC, Popoiu MC, Cimpean AM, David VL, Heredea R, Cerbu S and Boia ES. Expression of beta1 adrenergic receptor in vascular anomalies in children. *J Int Med Res*. 2021;49:3000605211047713.
27. Lawson ND and Weinstein BM. In vivo imaging of embryonic vascular development using transgenic zebrafish. *Dev Biol*. 2002;248:307-18.
28. Heckel E, Boselli F, Roth S, Krudewig A, Belting HG, Charvin G and Vermot J. Oscillatory Flow Modulates Mechanosensitive klf2a Expression through trpv4 and trpp2 during Heart Valve Development. *Curr Biol*. 2015;25:1354-61.
29. Wang Y, Kaiser MS, Larson JD, Nasevicius A, Clark KJ, Wadman SA, Roberg-Perez SE, Ekker SC, Hackett PB, McGrail M and Essner JJ. Moesin1 and Ve-cadherin are required in endothelial cells during in vivo tubulogenesis. *Development*. 2010;137:3119-28.
30. Jao LE, Wente SR and Chen W. Efficient multiplex biallelic zebrafish genome editing using a CRISPR nuclease system. *Proc Natl Acad Sci U S A*. 2013;110:13904-9.
31. Steele SL, Yang X, Debiais-Thibaud M, Schwerte T, Pelster B, Ekker M, Tiberi M and Perry SF. In vivo and in vitro assessment of cardiac beta-adrenergic receptors in larval zebrafish (Danio rerio). *J Exp Biol*. 2011;214:1445-57.
32. Mably JD, Chuang LP, Serluca FC, Mohideen MA, Chen JN and Fishman MC. santa and valentine pattern concentric growth of cardiac myocardium in the zebrafish. *Development*. 2006;133:3139-46.
33. Sehnert AJ, Huq A, Weinstein BM, Walker C, Fishman M and Stainier DY. Cardiac troponin T is essential in sarcomere assembly and cardiac contractility. *Nat Genet*. 2002;31:106-10.

34. Schwerte T, Uberbacher D and Pelster B. Non-invasive imaging of blood cell concentration and blood distribution in zebrafish Danio rerio incubated in hypoxic conditions in vivo. *J Exp Biol*. 2003;206:1299-307.
35. Langheinrich U, Vacun G and Wagner T. Zebrafish embryos express an orthologue of HERG and are sensitive toward a range of QT-prolonging drugs inducing severe arrhythmia. *Toxicol Appl Pharmacol*. 2003;193:370-82.
36. Gupta T and Mullins MC. Dissection of organs from the adult zebrafish. *J Vis Exp*. 2010.

Figure 1.

A

```
ATGGGAGACGGGCTACCGTCCGTAAACTACAGCAATGACTCTAAACGCGCCACGGTGGATCTTAACGTTTCAGAAC
AGTGGCTCGTGGGCATGGGAATCCTCATGGGTCTGATAGTGTTTGTCATTGTAGTGGGAAATATACTGGTTATAGT
CGCCATAGCGCGGAATCAGAGGCTCCAGACGCTCACCAATGTTTTCATCGTATCTCTGGCGTGCGCAGACCTCATC
ATGGGGTTACTGGTGGTGCCATTTGGCGCAGCCCTTGAGGTCAGAGGAGCCTGGATGTATGGATCGTTCTTCTGTG
AATTCTGGATATCTCTTGATGTACTTTGCGTCACGGCGAGCATCGAGACCCTGTGCGTAATTGCAATAGACAGGTA
TATCGCCATCATCTCTCCATTTCGCTATCAAAGCCTTTTAACAAAAGCACGAGCCAAGGTGGTGGTGTGTGCGGTG
TGGGCTATTTCAGCCCTGGTGTCGTTTCCCCCCATCCTAATGCACTGGTCCCAGGACAGCGAGGAGACATCGTGCT
ATGAAAATCCCGAGTGCTGTGACTTTGTCACCAACCGCGCATATGCCATCTCCTCGTCCATTATATCGTTTTACAT
CCCTTTAATAGTCATGATATTTGTCTATGCTAGAGTGTACAGAGAAGCCAAACAGCAGCTGAACAAGATCAACAAA
TGTGAGGGAAGGTTCTACAACAATCACGGTACAAACTGCAAACCAACCCGAAAACGGACCACCAAGATCCTGGCTT
TAAAAGAGCAGAAGGCTCTGAAAACGCTGGGAATAATCATGGGAACGTTCACTCTGTGTTGGCTGCCGTTCTTCAT
CGTGAACGTGGTGCGGGTGTTTTGCGCACAAGTGGTGGATAAGGAGCTCTTCGTCTTTTTGAACTGGCTGGGGTAC
GTCAACTCCGCATTTAATCCCATCATATACTGTCGGAGTCCCGACTTCAGAAAAGCCTTCAAAAGACTGTTGTGCT
GCCCGAGACAGGCGGACCGCAGGCTGCACGTGAGTTCGTGCGATCTGTCCCGCTGCACCGGAGGCTTTGGGAACTC
GATGGAGCAGAGTATGCTCGGGACGTGGTCGGACTGTAACGGCGCAGACAGCAGCGACTGCAGCCTGGAGAGAAAC
GGCAGGATGTCCCATTCAGAGTCTCAGCTGTAA
```

wt N C 390

adrb1$^{-/-}$ N C$_{18}$

B

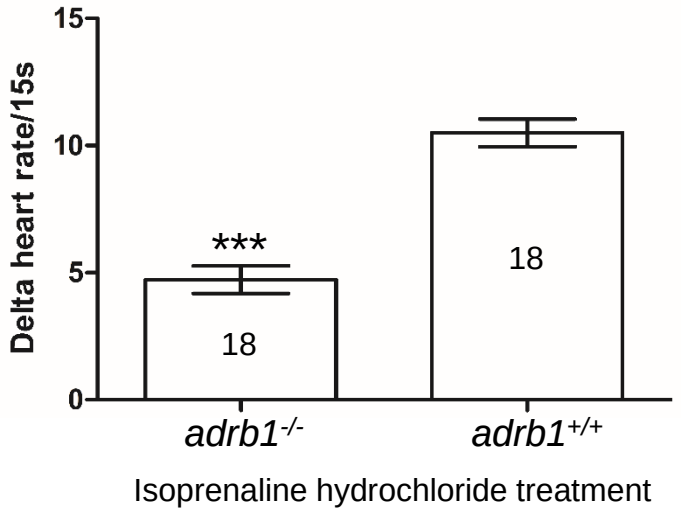

C

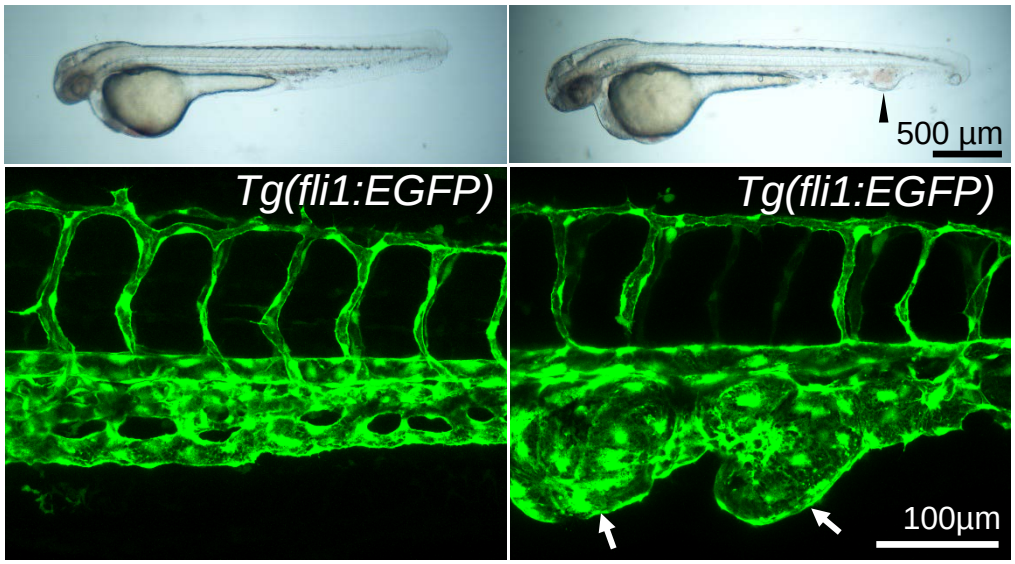

D

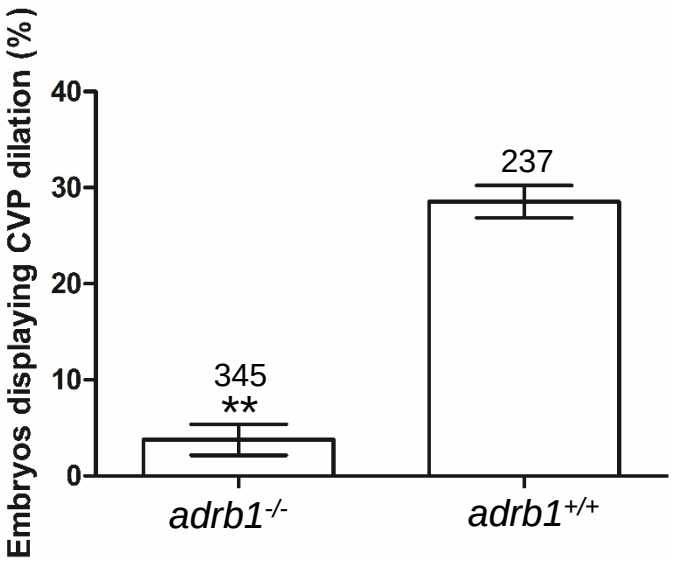

Figure 2.

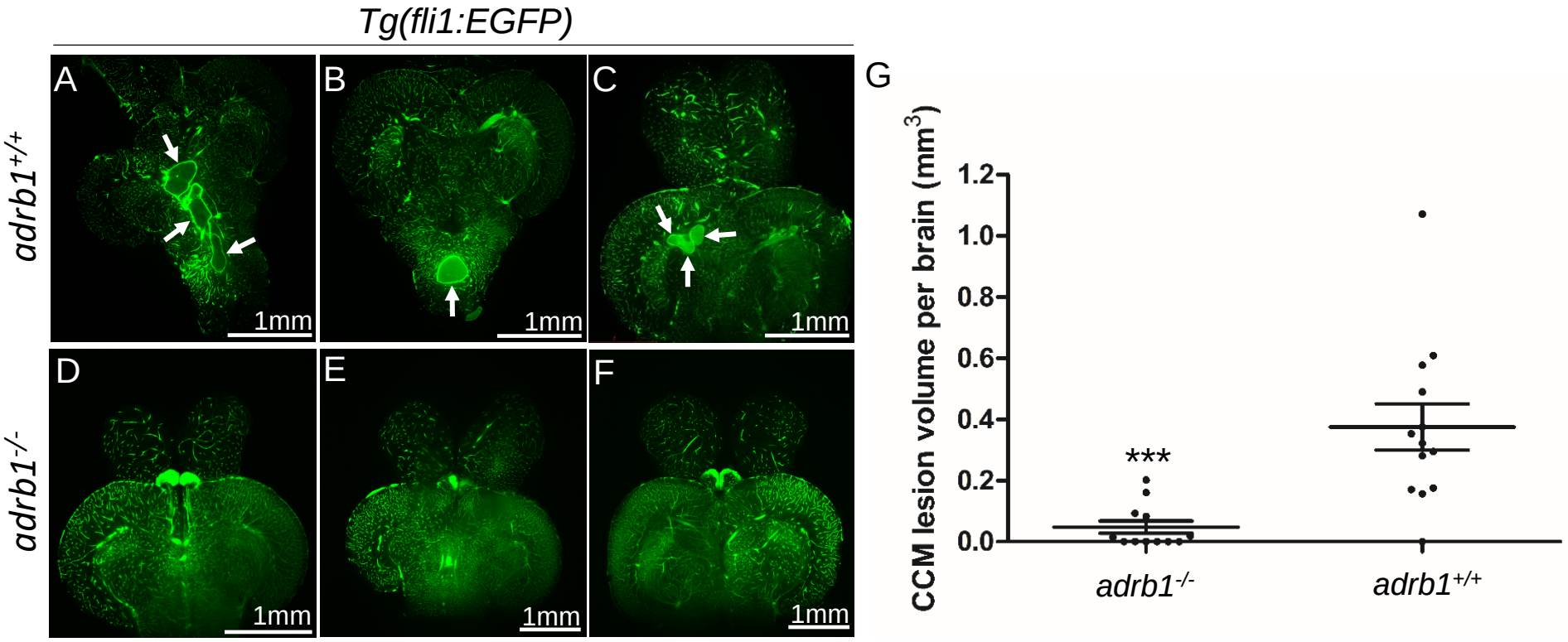
Tg(fli1:EGFP)
A
B
C
D
E
F
1mm
adrb1+/+
adrb1-/-
G
CCM lesion volume per brain (mm3)
1.2
1.0
0.8
0.6
0.4
0.2
0.0
***
adrb1-/-
adrb1+/+

Figure 3.

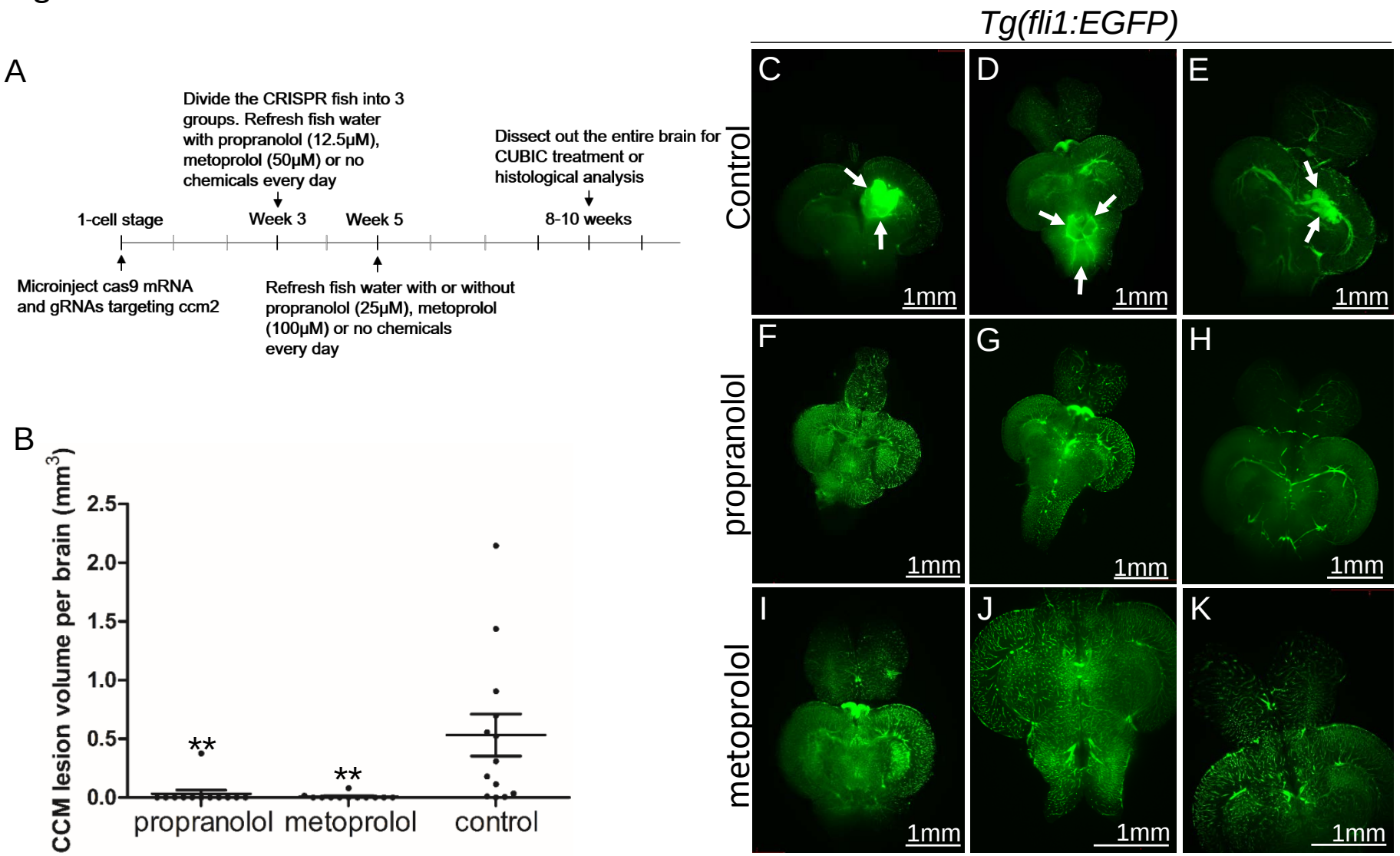
A
Divide the CRISPR fish into 3 groups. Refresh fish water with propranolol (12.5μM), metoprolol (50μM) or no chemicals every day
Dissect out the entire brain for CUBIC treatment or histological analysis
1-cell stage
Week 3
Week 5
8-10 weeks
Microinject cas9 mRNA and gRNAs targeting ccm2
Refresh fish water with or without propranolol (25μM), metoprolol (100μM) or no chemicals every day
B
CCM lesion volume per brain (mm3)
2.5
2.0
1.5
1.0
0.5
0.0
**
**
propranolol
metoprolol
control
Tg(fli1:EGFP)
Control
propranolol
metoprolol
C
D
E
F
G
H
I
J
K
1mm

Figure 4.

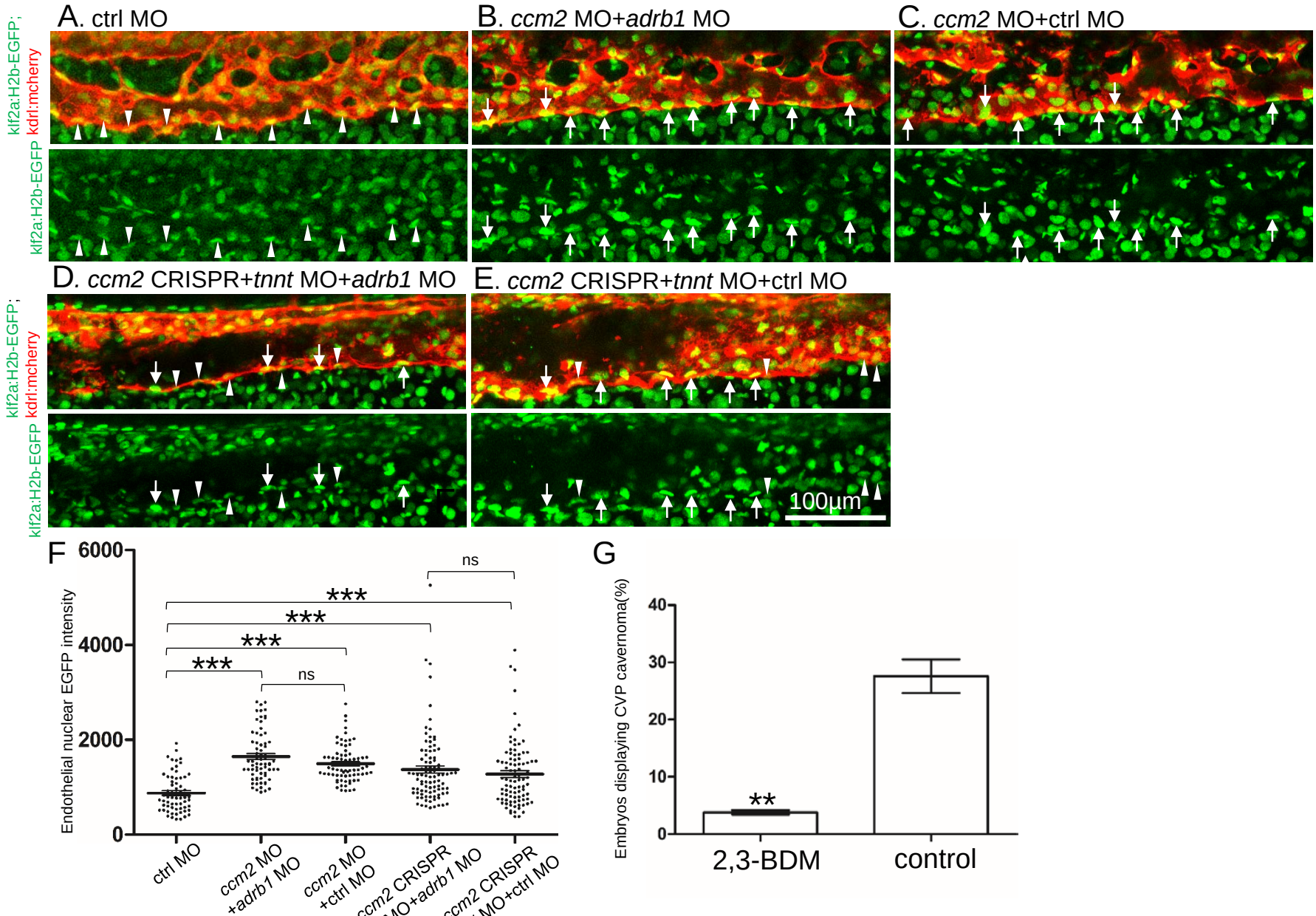
A. ctrl MO
B. ccm2 MO+adrb1 MO
C. ccm2 MO+ctrl MO
D. ccm2 CRISPR+tnnt MO+adrb1 MO
E. ccm2 CRISPR+tnnt MO+ctrl MO
klf2a:H2b-EGFP; kdrl:mcherry
klf2a:H2b-EGFP
100μm
F
Endothelial nuclear EGFP intensity
6000
4000
2000
0
***
***
***
***
ns
ns
ctrl MO
ccm2 MO +adrb1 MO
ccm2 MO +ctrl MO
ccm2 CRISPR +tnnt MO+adrb1 MO
ccm2 CRISPR +tnnt MO+ctrl MO
G
Embryos displaying CVP cavernoma(%)
40
30
20
10
0
**
2,3-BDM
control